ISSN 0020-1685, Inorganic Materials, 2021, Vol. 57, No. 9, pp. 906–912. © Pleiades Publishing, Ltd., 2021.
Russian Text © The Author(s), 2021, published in Neorganicheskie Materialy, 2021, Vol. 57, No. 9, pp. 954–961.

Porous Silica Particles Modified in a $NH_3 + H_2O + H_2O_2$ Mixture: Structure, Filling with Cobalt Oxide, and Catalytic Activity for CO Conversion

D. A. Eurov[a], *, D. A. Kirilenko[a], M. V. Tomkovich[a], T. N. Rostovshchikova[b], M. I. Shilina[b], O. V. Udalova[c], and D. A. Kurdyukov[a]

[a] *Ioffe Institute, St. Petersburg, 194021 Russia*

[b] *Moscow State University, Moscow, 119991 Russia*

[c] *Semenov Federal Research Center for Chemical Physics, Russian Academy of Sciences, Moscow, 119334 Russia*

**e-mail: edan@mail.ru*

Received April 1, 2021; revised May 20, 2021; accepted May 21, 2021

Abstract—Silica particles containing large mesopores (5–25 nm in size) and micropores (0.6–2 nm in size) have been prepared by chemical etching of spherical micro- and mesoporous silica particles in an ammonia + water + hydrogen peroxide mixture. The specific surface area and pore volume of the particles are 510 m^2/g and 0.8 cm^3/g, respectively. Using capillary impregnation, we have synthesized Co_3O_4 (2–4 wt %) in pores of the particles. The composition and structure of the resultant materials have been studied. The Co_3O_4/SiO_2 composite particles have been shown to be stable and exhibit catalytic activity for the CO oxidation process.

Keywords: spherical particles, nanoporous silica, cobalt oxide, catalysis, carbon monoxide

DOI: 10.1134/S0020168521090053

INTRODUCTION

Owing to its attractive properties, such as a large specific surface area, large pore volume, variable pore morphology and size, chemical and thermal stability, and biocompatibility, mesoporous silica has found application in catalysis [1], adsorption [2], molecular separation [3], biomedicine [4], optoelectronics [5], and other areas. Of particular interest are monodisperse spherical mesoporous silica particles. When used, for example, in catalysis or chromatography, such particles can form the closest packing, which in turn ensures a uniform mass transport rate (in pores and outside of the particles) [6]. In addition, monodisperse spherical mesoporous silica particles are potentially attractive for use in biomedical applications as carriers in drug delivery systems [7–9].

Spherical mesoporous silica particles are typically synthesized via the hydrolysis of silicon-containing precursors on the surface of micelles formed by surfactant molecules. The surfactant molecule length determines the pore size in the synthesized particles. In most cases, cetyltrimethylammonium bromide (CTAB) or decyltrimethylammonium bromide (DTAB) is used as a pore former, and the resulting silica particles contain mesopores no more than 3 nm in average size.

A variety of technological and medical applications require particles containing larger pores. In particular, previous work [5] has demonstrated the feasibility of using silica particles containing mesopores up to 15 nm in size as a matrix for dispersing carbon quantum dots, promising as phosphors for white light emitting diodes. Particles containing through pores more than 8 nm in size and ensuring fast mass transport are optimal for highly efficient liquid chromatography [10]. As shown by Horcajada et al. [9], if silica particles are used for drug delivery, a larger mesopore size ensures a larger amount of loaded and delivered drug per unit surface area of the carrier and a higher drug release rate.

As a rule, two approaches are used to increase the mesopore size in silica particles. In one of them, an organic compound (for example, trimethylbenzene), whose molecules become incorporated into surfactant micelles, is added to the reaction mixture [11, 12]. The other approach employs surfactants with a longer hydrophobic part [12, 13]. Both approaches influence the particle synthesis process and, as a consequence, the parameters (size and shape) of the particles. This can be avoided using postsynthetic treatment of particles, for example, etching of monodisperse spherical mesoporous silica particles (with a pore diameter of 3 nm) in an alcohol–water–ammonia medium in an autoclave at 120°C [14]. After such treatment, the size and shape of the particles remain unchanged. At the

same time, they contain large mesopores, more than 10 nm in size, and macropores up to 100 nm in size.

In this paper, we report an approach for the preparation of spherical silica particles containing large mesopores (up to 25 nm in size). Such particles were prepared by wet chemical etching of micro- and mesoporous SiO_2 particles in an ammonia + water + hydrogen peroxide mixture under ordinary conditions. The proposed method makes it possible to increase the average mesopore diameter from 2.5 to ~20 nm, while maintaining a large specific surface area and pore volume in the particles. The pores of the resultant particles were filled with cobalt oxide, Co_3O_4. Cobalt oxides are known to be effective catalysts for oxygen oxidation of carbon monoxide [15], capable of competing with noble metals. However, their use is limited by their insufficient stability under catalysis conditions. Stabilization of cobalt oxide in the pores of the synthesized mesoporous silica ensured its stability in catalytic oxidation of CO.

EXPERIMENTAL

We used the following substances and reagents: CTAB, $C_{16}H_{33}N(CH_3)_3Br$ (99+%, Acros); aqueous ammonia, NH_3 (24 wt % NH_3, ≥99.99%); ethanol, C_2H_5OH (95 wt %); deionized water, H_2O (10 MΩ); tetraethyl orthosilicate (TEOS), $Si(OC_2H_5)_4$ (99+%, Acros); methacryloxypropyltrimethoxysilane (MPTMOS), $Si(OC_2H_5)_4$ (99+%, Acros); hydrochloric acid, HCl (37 wt %, ≥99.99%); hydrogen peroxide, H_2O_2 (30–35 wt %, ≥99.99%); and cobalt nitrate hexahydrate, $Co(NO_3)_2{\cdot}6H_2O$ (98%, Aldrich).

Spherical micro- and mesoporous silica particles ranging in pore size from 0.6 to 4 nm were synthesized by a previously developed technique via basic hydrolysis of silicon-containing precursors (TEOS and MPTMOS) in a $NH_3 + H_2O + C_2H_5OH$ + CTAB mixture [16, 17]. The (TEOS + 20 mol % MPTMOS) : NH_3 : H_2O : C_2H_5OH : CTAB molar ratio was 1 : 60 : 370 : 230 : 0.2, and the weight of the solution was 1 kg. The temperature of the reaction mixture was 60°C, and the synthesis time was 2 h. To remove organics, the synthesized particles were washed in an ethanolic HCl solution (0.01 M) and then annealed in flowing O_2 at a temperature of 400°C for 5 h. The specific surface area and pore volume of the synthesized particles were 1600 m^2/g and 0.55 cm^3/g, respectively [16].

To modify the pore structure (increase the mesopore size), 50 mL of a freshly prepared aqueous solution of H_2O_2 (3 M) and NH_3 (10 M) was added to a glass beaker containing a weighed amount (0.5 g) of silica particles. The resultant suspension was heated with stirring to a temperature of 65°C, held there for 1 h, and then cooled to room temperature in air. After this treatment, the particles were washed three times with deionized water and dried at a temperature of 100°C.

Co_3O_4 was introduced into the pores of the particles in several steps. In the first step, a weighed amount of silica particles was impregnated with an aqueous 2 M $Co(NO_3)_2{\cdot}6H_2O$ solution under ordinary conditions, and the particles were dried at 70°C. Next, the temperature of the sample was raised to 300°C at a rate of 10°C/min. After that, it was heat-treated at 300°C for 3 h under ordinary conditions. We prepared two samples, containing 2 and 4 wt % Co_3O_4, as evaluated from the weight ratio of the silica particles to cobalt nitrate.

The pore structure of the particles was studied at a temperature of 77 K using a Micromeritics ASAP 2020 analyzer and nitrogen as an adsorbate. The pore size was calculated using built-in software and nonlocal density functional theory (NDFT). The specific surface area of the particles was evaluated using BET analysis, and the specific pore volume was determined at a relative pressure $p/p_0 = 0.994$. The particles were examined by transmission electron microscopy (TEM) on a JEOL JEM-2100F (accelerating voltage, 200 kV; point-to-point resolution, 0.19 nm) equipped with an energy dispersive X-ray spectrometer system.

The catalytic activity of the Co_3O_4/SiO_2 particles for catalytic carbon monoxide oxidation reaction was studied in flow-through mode at temperatures in the range 50–250°C in two to four heating–cooling cycles. Before testing, the samples were heated in flowing He at 370°C for 30 min. The temperature was controlled by a Ursamar-RK42 controller (Germany). The composition of the starting mixture was 1 vol % CO, 1 vol % O_2, and 98 vol % He. The reaction mixture was analyzed for CO and CO_2 using a Kristall 2000 chromatograph. The chromatographic analysis conditions were as follows: thermal conductivity detector, 1-m column packed with Porapak–Q, column temperature of 30°C, and carrier gas (He) flow rate of 10 cm^3/min. The data thus obtained were analyzed using Ekokhrom software.

RESULTS AND DISCUSSION

Consider one possible mechanism of the formation of large mesopores (10–25 nm in size) during etching of micro- and mesoporous silica particles in a $NH_3 + H_2O + H_2O_2$ mixture. Initially, the particles consist of clusters of densely packed SiO_2 tubes having micropores 0.6 to 2 nm in size in their walls and between them [16, 17]. The average inner diameter of the tubes is ~2.5 nm; the thickness of their walls is ~0.5 nm; and the cluster size, equal to the tube length, is 10–15 nm [16]. It seems likely that large mesopores are formed through coalescence of neighboring mesopores in a cluster, that is, through elimination of the walls between neighboring SiO_2 tubes (Fig. 1). Previously, a

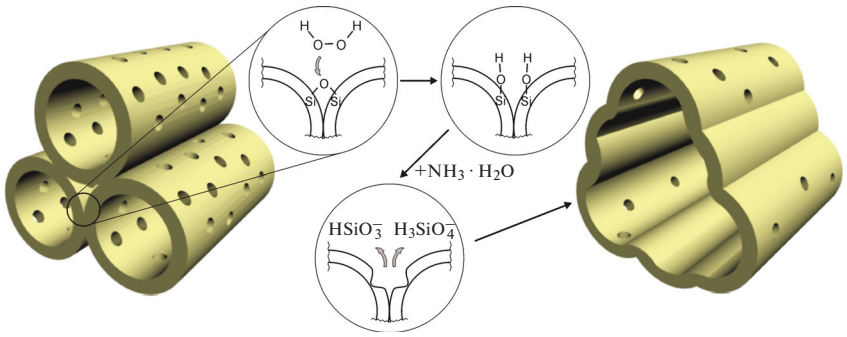

Fig. 1. Schematic of the process underlying the formation of large mesopores during etching of micro- and mesoporous silica (SiO_2) particles.

similar process was observed during etching of mesoporous silica particles in ammonia at 120°C in an autoclave [14]. Silica dissolution begins in places with the highest chemical activity, namely, at silanol groups. In effect, because of the very large specific surface area (1600 m^2/g according to BET measurements [16]), micro- and mesoporous silica is closer in composition to polysilicic acid than to silicon dioxide. Obviously, the largest number of silanol groups is located on micropore walls, because they have the smallest curvature radius and it is in these places where the formation of dangling bonds in the silicon–oxygen framework and single silanol groups is most likely (because of the steric hindrances). The presence of hydrogen peroxide in the etchant further raises the surface density of silanol groups. As shown by Żegliński et al. [18], H_2O_2 molecules are adsorbed by not only silanol groups but also siloxane bonds on the surface of silica. Interaction of H_2O_2 decomposition products with –Si–O–Si– can lead to the formation of two –Si–OH groups (Fig. 1).

Interaction of OH^-, H_2O, and NH_4^+ with silica leads to the formation of $HSiO_3^-$ and $H_3SiO_4^-$ ions. It seems likely that the hydrated hydrogen silicate ions then diffuse to the outer boundaries of the cluster (Fig. 1) where hydrated amorphous SiO_2 is again formed. The walls of the forming larger pores are thicker and have a larger curvature radius, so their surface is less chemically active.

The particles were found to retain spherical shape after etching (Fig. 2). TEM images show pores (light areas) ~10 to 20 nm in size. A TEM image of the article surface demonstrates roughness (~20–30 nm) comparable to the size of large pores. Figure 3 shows a 77-K nitrogen adsorption isotherm of the particles after etching (Fig. 3a, curve *1*). The TEM results correlate with nitrogen adsorption porosimetry data. The adsorption isotherm exhibits hysteresis at relative pressures in the range $0.5 \le p/p_0 \le 1.0$, which is due to capillary condensation in large mesopores. NDFT calculations give a broad pore size distribution, from a fraction of a nanometer to several tens of nanometers. It seems likely that the pores 0.6 to 2 nm in size were present in the initial structure of the particles before etching and were located in the walls of the large pores (Fig. 1). The calculated specific surface area and pore volume were 513 m^2/g (BET analysis) and 0.79 cm^3/g, respectively. It seems likely that it is owing to the more active surface of micro- and mesoporous silica that its etching was possible under substantially "milder" conditions compared to what was reported by Stovpiaga et al. [14] (120°C in an autoclave), which led to the formation of a more porous material. In particular, the pore volume of the particles after etching was ~0.8 cm^3/g, exceeding the pore volume of the starting micro- and mesopores particles by ~0.15 cm^3/g. It seems likely that some of the hydrogen silicate ions passed from pores to the solution without forming $SiO_2 \cdot H_2O$ again.

Table 1. Temperatures of 50 and 90% CO conversion in two sequential heating–cooling cycles on samples with different Co_3O_4 concentrations

wt % Co_3O_4	Cycle	t_{50}, °C		t_{90}, °C	
		heating	cooling	heating	cooling
4	*1*	160	162	186	187
	2	165	162	191	187
2	*1*	158	160	180	182
	2	163	160	183	181

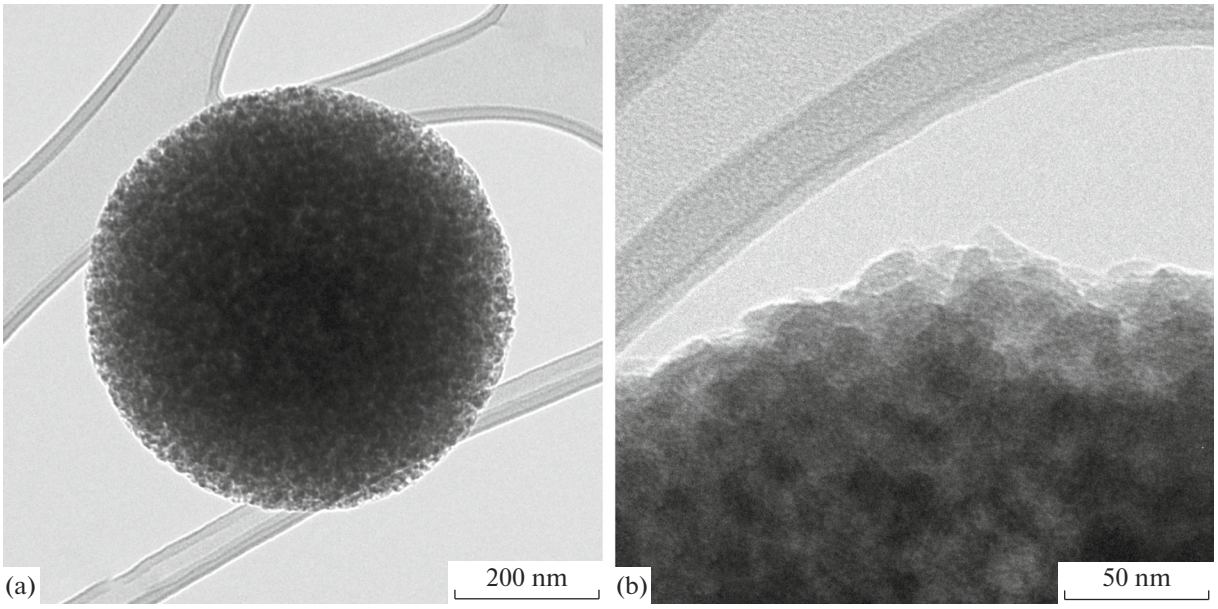

Fig. 2. TEM images of (a) a SiO_2 particle and (b) its surface after treatment with a $NH_3 + H_2O + H_2O_2$ mixture.

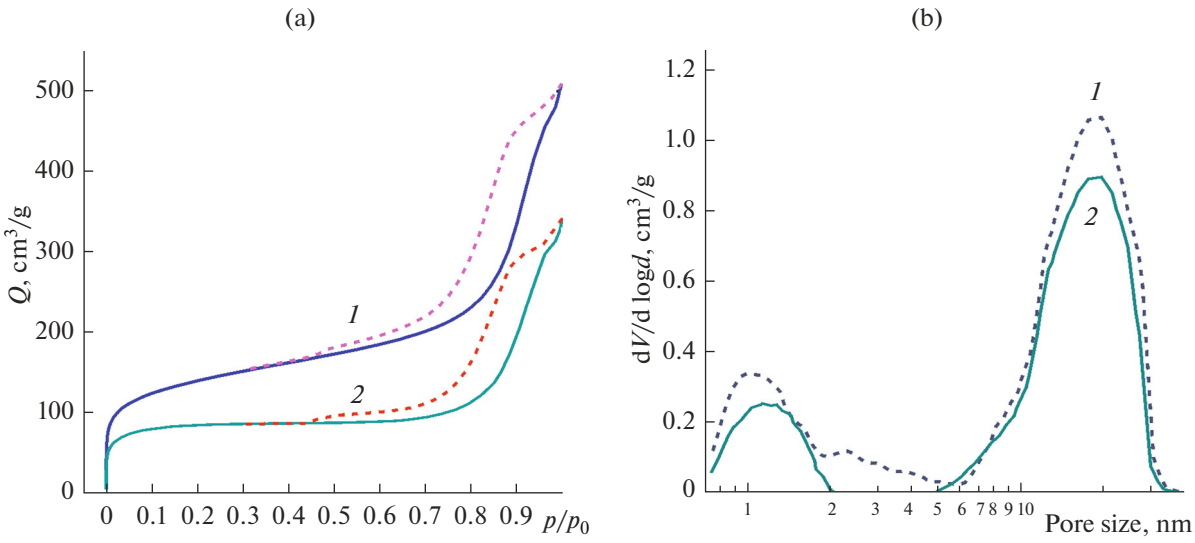

Fig. 3. (a) 77-K nitrogen adsorption isotherms and (b) pore size distribution obtained by NDFT calculations for (*1*) SiO_2 and (*2*) Co_3O_4/SiO_2 particles.

Figure 4a shows a TEM image of the particles after the incorporation of Co_3O_4 via capillary impregnation. Here and in what follows, we present results of structural studies for the Co_3O_4/SiO_2 sample containing 4% cobalt oxide. It is seen in the image that the composite particles appear darker than the starting particles (Fig. 2a), probably because they contain Co, a heavier element responsible for a stronger electron absorption. The enlarged image of the surface region in Fig. 4b shows a crystallite (dark region). The interplanar spacing observed in it corresponds to the d_{311} = 0.25 nm of Co_3O_4. The TEM images show Co_3O_4 crystallites a few to tens of nanometers in size. The selective area electron diffraction pattern of the composite particles (Fig. 4c) shows diffraction reflections from Co_3O_4 (JCPDS card no. 00-042-1467). We are thus led to conclude that the major crystalline phase is Co_3O_4. At the same time, the formation of amorphous cobalt oxide or silicate, especially in the micropores of the silica particles, cannot be completely ruled out. The elemental analysis data confirm the presence of cobalt and the absence of other elements as impurities

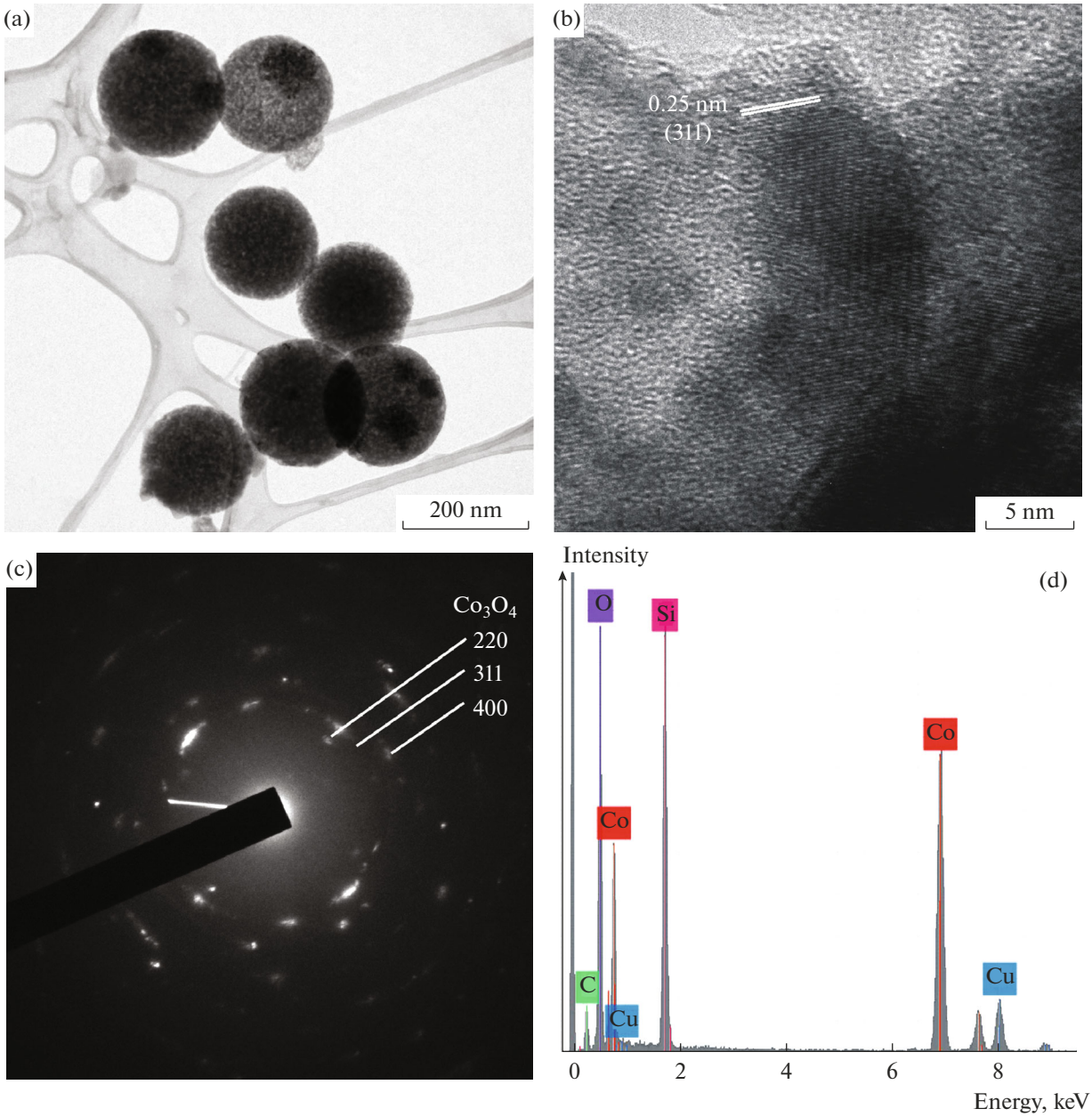

Fig. 4. (a) TEM and (b) high-resolution TEM images, (c) selective area electron diffraction pattern, and (d) energy dispersive X-ray spectrum of the Co_3O_4/SiO_2 particles (in panels b and c, we indicate a characteristic interplanar spacing and the position of diffraction reflections from Co_3O_4, respectively).

in the composition of the particles (Fig. 4d). The copper signal observed in the X-ray spectrum originated from the copper grid supporting the TEM specimen. According to the nitrogen adsorption porosimetry data (Fig. 3), the specific surface area and pore volume were 410 m^2/g and 0.61 cm^3/g, respectively.

The catalytic activity of the Co_3O_4/SiO_2 composite particles containing 2 and 4 wt % Co_3O_4 was studied using the catalytic oxidation of carbon monoxide in a $CO + O_2 + He$ mixture as an example. Figure 5 shows temperature dependences of CO conversion obtained using Co_3O_4/SiO_2 (4 wt % Co_3O_4) particles in two sequential heating–cooling cycles. It is seen that 50% CO conversion was reached at a temperature of 160°C, and 100% conversion, at 210°C. The characteristic temperatures t_{50} and t_{100} varied little in repeated tests of the samples. It is seen from Table 1 that, in the case of the sample with the lower Co_3O_4 content (2 wt %), we obtained similar or even slightly lower temperatures of 50 and 90% CO conversion. This seems to be related to the narrower particle size distribution of the Co_3O_4 in the sample with the lower Co_3O_4 concentration.

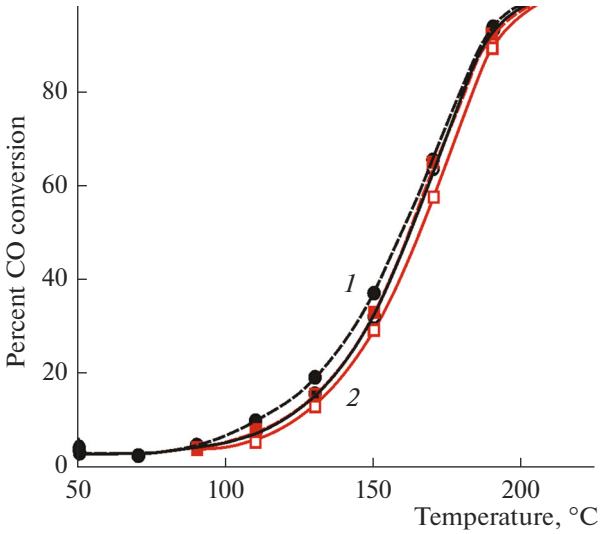

Fig. 5. CO conversion as a function of reaction temperature for Co_3O_4/SiO_2 particles containing 4 wt % cobalt oxide (the solid lines and open data points refer to heating, and the dashed lines and filled data points refer to cooling): (*1*) first and (*2*) second heating–cooling cycles.

In the case of cobalt oxides supported on γ- or α-Al_2O_3, 100% CO conversion in an excess of oxygen can be reached at temperatures above 200 and 300°C, respectively [19, 20]. In the case of Co_3O_4/MCM-41 catalysts containing 6% Co_3O_4, which are closer in composition to the samples synthesized by us, 50 and 100% conversions can be reached at temperatures from 180 to 152 and from 285 to 222°C [21]. Note that the above CO conversion data were also obtained for a CO-rich reaction mixture with a large oxygen excess (4% CO, 20% O_2, and He), which would be expected to contribute to more effective oxidation. No data on the feasibility of reusing such samples were presented in the papers in question. Since the oxidation of CO is rather sensitive to process conditions (concentrations of and relationships between the components of the reaction mixture, carrier gas flow rate, reactor design, and others), adequate comparison of data is only possible for catalysts tested under identical conditions. In the case of one promising catalytic system based on Co-modified zeolites containing 2.8 wt % cobalt oxide, the temperature t_{50} determined under conditions similar to those in this study was 190°C during heating and then decreased to 170°C when the catalyst was reused during cooling [22]. The use of the Co_3O_4/SiO_2 particles synthesized in this work ensures t_{50} in the range 160–165°C. The catalysts remained effective when reused.

CONCLUSIONS

We have developed a technique for the preparation of particles containing large mesopores (more than 10 nm in size) via chemical etching of micro- and mesoporous particles in an ammonia + water + hydrogen peroxide mixture and proposed a mechanism of formation of large mesopores through coalescence of neighboring nanometer-sized pores via reversible silica dissolution and the formation of hydrogen silicate ions. TEM and nitrogen adsorption porosimetry data demonstrate that the resultant particles are spherical in shape and contain mesopores (5–25 nm in size) and micropores (0.6–2 nm in size). The specific surface area and pore volume of the particles are 510 m^2/g and 0.79 cm^3/g, respectively.

Using capillary impregnation, we have synthesized Co_3O_4 (2–4 wt %) in pores of the particles. The Co_3O_4/SiO_2 composite particles have been shown to have a large specific surface area and pore volume (up to 410 m^2/g and 0.61 cm^3/g, respectively). We have studied the catalytic activity of the composite articles for the oxidation of carbon monoxide with oxygen. According to their effectiveness, the synthesized Co_3O_4/SiO_2 particles are comparable to or even slightly surpass known catalysts based on nanoporous oxide carriers and Co_3O_4. The t_{50} of the samples containing 2 and 4 wt % Co_3O_4 approaches 160°C, and they ensure complete CO conversion at temperatures near 200°C. An important advantage of the proposed composite materials is that their effectiveness remains unchanged when they are used repeatedly.

ACKNOWLEDGMENTS

In our transmission electron microscopy work, we used equipment at the Materials Engineering and Diagnosis in Advanced Technologies Federal Shared Research Facilities Center.

FUNDING

The synthesis and physicochemical characterization of the materials were supported by the Russian Federation Ministry of Science and Higher Education s part of the state research target no. 0040-2019-0012. The catalytic tests were supported through state research targets, theme nos. AAAA-A21-121011590090-7 and 0082-2019-0011: Fundamental relationships in heterogeneous and homogeneous catalysis.

REFERENCES

1. Verma, P., Kuwahara, Y., Mori, K., Raja, R., and Yamashita, H., Functionalized mesoporous SBA-15 silica: recent trends and catalytic applications, *Nanoscale,* 2020, vol. 12, pp. 11333–11363. https://doi.org/10.1039/D0NR00732C
2. Ramasamy, D.L., Puhakka, V., Iftekhar, S., Wojtuś, A., Repo, E., Ben Hammouda, S., Iakovleva, E., and Sillanpää, M., N- and O-ligand doped mesoporous silica-chitosan hybrid beads for the efficient, sustainable and selective recovery of rare earth elements (REE) from

acid mine drainage (AMD): understanding the significance of physical modification and conditioning of the polymer, *J. Hazard. Mater.,* 2018, vol. 348, pp. 84–91. https://doi.org/10.1016/j.jhazmat.2018.01.030

3. Yang, J., Lin, G.-S., Mou, C.-Y., and Tung, K.-L., Mesoporous silica thin membrane with tunable pore size for ultrahigh permeation and precise molecular separation, *ACS Appl. Mater. Interfaces,* 2020, vol. 12, pp. 7459–7465. https://doi.org/10.1021/acsami.9b21042
4. Wang, Y., Zhao, Q., Han, N., Bai, L., Li, J., Liu, J., Che, E., Hu, L., Zhang, Q., Jiang, T., and Wang, S., Mesoporous silica nanoparticles in drug delivery and biomedical applications, *Nanomed.: NBM,* 2015, vol. 11, pp. 313–327. https://doi.org/10.1016/j.nano.2014.09.014
5. Eurov, D.A., Kurdyukov, D.A., Medvedev, A.V., Kirilenko, D.A., Tomkovich, M.V., and Golubev, V.G., Micro-mesoporous submicron silica particles with pore size tunable in a wide range: synthesis, properties and prospects for LED manufacturing, *Nanotechnology,* 2021, vol. 32, paper 215604. https://doi.org/10.1088/1361-6528/abe66e
6. Unger, K.K., Kumar, D., Grun, M., Buchel, G., Ludtke, S., Adam, Th., Schumacher, K., and Renker, S., Synthesis of spherical porous silicas in the micron and submicronsize range: challenges and opportunities for miniaturized high-resolution chromatographic and electrokinetic separations, *J. Chromatogr., A,* 2000, vol. 892, pp. 47–55. https://doi.org/10.1016/s0021-9673(00)00177-1
7. Asefa, T. and Tao, Z., Biocompatibility of mesoporous silica nanoparticles, *Chem. Res. Toxicol.,* 2012, vol. 25, pp. 2265–2284. https://doi.org/10.1021/tx300166u /
8. Vivero-Escoto, J.L., Slowing, I.I., Trewyn, B.G., and Lin, V.S.-Y., Mesoporous silica nanoparticles for intracellular controlled drug delivery, *Small,* 2010, vol. 6, pp. 1952–1967. https://doi.org/10.1002/smll.200901789
9. Horcajada, P., Rámila, A., Pérez-Pariente, J., and Vallet-Regi, M., Influence of pore size of MCM-41 matrices on drug delivery rate, *Microporous Mesoporous Mater.,* 2004, vol. 68, pp. 105–109. https://doi.org/10.1016/j.micromeso.2003.12.012
10. Unger, K.K., Skudas, R., and Schulte, M.M., Particle packed columns and monolithic columns in high-performance liquid chromatography—comparison and critical appraisal, *J. Chromatogr., A,* 2008, vol. 1184, pp. 393–415. https://doi.org/10.1016/j.chroma.2007.11.118
11. Beck, J.S., Vartuli, J.C., Roth, W.J., Leonowicz, M.E., Kresge, C.T., Schmitt, K.D., Chu, T.W.C., Olson, D.H., Sheppard, E.W., McCullen, S.B., Higgins, J.B., and Schlenker, J.L., A new family of mesoporous molecular sieves prepared with liquid crystal templates, *J. Am. Chem. Soc.,* 1992, vol. 114, pp. 10834–10843. https://doi.org/10.1021/ja00053a020
12. Jana, S.K., Mochizuki, A., and Namba, S., Progress in pore-size control of mesoporous MCM-41 molecular sieve using surfactant having different alkyl chain lengths and various organic auxiliary chemicals, *Catal. Surv.,* 2004, vol. 8, pp. 1–13. https://doi.org/10.1023/B:CATS.0000015110.85694.d9
13. Knežević, N.Ž. and Durand, J.-O., Large pore mesoporous silica nanomaterials for application in delivery of biomolecules, *Nanoscale,* 2015, vol. 7, pp. 2199–2209. https://doi.org/10.1039/C4NR06114D
14. Stovpiaga, E.Yu., Grudinkin, S.A., Kurdyukov, D.A., Kukushkina, Yu.A., Nashchekin, A.V., Sokolov, V.V., Yakovlev, D.R., and Golubev, V.G., Monodisperse spherical meso–macroporous silica particles: synthesis and adsorption of biological macromolecules, *Phys. Solid State,* 2016, vol. 58, no. 11, pp. 2339–2344. https://doi.org/10.1134/S1063783416110342
15. Royer, S. and Duprez, D., Catalytic oxidation of carbon monoxide over transition metal oxides, *ChemCatChem,* 2011, vol. 3, pp. 24–65. https://doi.org/10.1002/cctc.201000378
16. Kurdyukov, D.A., Eurov, D.A., Kirilenko, D.A., Kukushkina, J.A., Sokolov, V.V., Yagovkina, M.A., and Golubev, V.G., High-surface area spherical micro-mesoporous silica particles, *Microporous Mesoporous Mater.,* 2016, vol. 223, pp. 225–229. https://doi.org/10.1016/j.micromeso.2015.11.018
17. Kurdyukov, D.A., Eurov, D.A., Sokolov, V.V., and Golubev, V.G., Tailoring the size and microporosity of Stöber silica particles, *Microporous Mesoporous Mater.,* 2018, vol. 258, pp. 205–210. https://doi.org/10.1016/j.micromeso.2017.09.017
18. Żegliński, J., Piotrowski, G.P., and Piękoś, R., A study of interaction between hydrogen peroxide and silica gel by FTIR spectroscopy and quantum chemistry, *J. Mol. Struct.,* 2006, vol. 794, pp. 83–91. https://doi.org/10.1016/j.molstruc.2006.01.043
19. Zhang, L., Dong, L., Yu, W., Liu, L., Deng, Y., Liu, B., Wan, H., Gao, F., Sun, K., and Dong, L., Effect of cobalt precursors on the dispersion, reduction, and CO oxidation of CoO_x/γ-Al_2O_3 catalysts calcined in N_2, *J. Colloid Interface Sci.,* 2021, vol. 355, pp. 464–471. https://doi.org/10.1016/j.jcis.2010.11.076
20. Hattori, M., Nakakura, S., Katsui, H., Goto, T., and Ozawa, M., High CO reactivity of cobalt oxide catalyst deposited on alumina powders by rotary chemical vapor deposition, *Mater. Lett.,* 2021, vol. 284, paper 128922. https://doi.org/10.1016/j.matlet.2020.128922/
21. Hassan, H.M.A., Betiha, M.A., Elshaarawy, R.F. M., and Samy El-Shall, M., Promotion effect of palladium on Co_3O_4 incorporated within mesoporous MCM-41 silica for CO oxidation, *Appl. Surf. Sci.,* 2017, vol. 402, pp. 99–107. https://doi.org/10.1016/j.apsusc.2017.01.061
22. Shilina, M.I., Rostovshchikova, T.N., Nikolaev, S.A., and Udalova, O.V., Polynuclear Co-oxo cations in the catalytic oxidation of CO on Co-modified ZSM-5 zeolites, *Mater. Chem. Phys.,* 2019, vol. 223, pp. 287–298. https://doi.org/10.1016/j.matchemphys.2018.11.005

Translated by O. Tsarev